This contains supplementary information about:
marine DBC stable isotopes,
model model methods
SFigure 1-2
STable 1

Understanding the stable carbon isotopic composition of oceanic DBC

The stable carbon isotopic composition of oceanic DBC[1] may appear to result from large contributions of DBC derived from charred, 13C-enriched C_4 plants[2]. Although this explanation would seem feasible, given that 50% of charcoal is produced in savannah environments, we do not observe a ^{13}C-enriched isotopic signature for DBC in major rivers[1], including those which drain large areas of fire-affected savannah[3]. One study has shown that atmospherically-deposited wildfire ash leaches DBC with a ^{13}C-depleted isotopic signature, however, the atmospheric deposition of ash and smoke to coastal surface waters did not supply DBC in sufficient quantities to meaningfully shift marine DBC $\delta^{13}C$ signatures[4]. The inferred presence of a marine source for oceanic DBC also assumes that DBC $\delta^{13}C$ values are consistent with that of their unburned biomass source and that the isotopic composition of DBC is not fractionated (or altered) during riverine and coastal transit. On average, PBC has lower $\delta^{13}C$ values relative to bulk POC and DOC, which suggest some degree of isotopic fractionation occurs during soil organic matter production, biomass burning, and/or transport[5]. Furthermore, although we expect DBC $\delta^{13}C$ values to be consistent with the isotopic composition of BC in the original particulate charcoals, fractionation of DBC during leaching has not been directly tested. Photodegradation is identified as a major loss mechanism for DBC in sunlit surface waters[6] , therefore photo-fractionation of DBC $\delta^{13}C$ values is possible and may partially explain the observed isotopic offset between riverine and oceanic endmembers. A large input of polyaromatic hydrocarbons and other semi-volatile aromatic-like compounds by diffusive air–water exchange is a newly identified source of DBC to oceanic surface waters[7], which could contribute to the $\delta^{13}C$ signatures observed for oceanic DBC, but the isotopic composition of these semi-volatile aromatic-like compounds that are quantified and characterized as DBC is unknown. It was recently discovered that anaerobic methanotrophs are capable of synthesizing elemental carbon[8]. Therefore, marine biotic sources of condensed aromatic material that is characterized as DBC and PBC are also possible.

7-component box model

We use a model dividing the ocean into 7 boxes, adapted from[9,10], to simulate age and concentration of two DBC pools in the ocean. The model simulates an overturning circulation with water exchange between surface and subsurfaces boxes as detailed in Toggweiler et al. 1998, but the intensity of water exchange between model boxes has been modified here to achieve an ideal water mass age of 1200 years as in[11,12] (Supplementary Fig. 1). This modification is needed in order to obtain a reasonable water mass age that impacts the ageing of DBC as it travels along the overturning circulation. The model is spun up for 30000 years until stabilization of DBC concentration and age, and the last year is used for evaluation. The model is solved using the ode45-solver in Matlab (R2018a).

DBC concentration of the fast overturning pool DBC_1 and the slowly-overturning DBC pool DBC_2 is computed as follows, including various sources γ from rivers, sediments and aerosol, as well as sinks following a first-order kinetic and photodegradation:

$$\frac{dDBC_1}{dt} = +\varepsilon \cdot \gamma_{river} + \gamma_{sediment1} + \gamma_{aerosol1} - k_1 \cdot [DBC_1] - \lambda_{UV} \cdot [DBC_1] \qquad (1)$$

$$\frac{dDBC_2}{dt} = +(1-\varepsilon) \cdot \gamma_{river2} + \gamma_{sediment2} + \gamma_{aerosol2} - k_2 \cdot [DBC_2] - \lambda_{UV} \cdot [DBC_2] \qquad (2)$$

$$DBC = DBC_1 + DBC_2 \qquad (3)$$

DBC age A_{DBC} is computed individually for both pools, and a concentration-weighted average is computed for total DBC age:

$$\frac{dA_{DBC1}}{dt} = 1 + \sum\nolimits_{river,sediment,aerosol} \frac{\gamma}{A_{DBC1}} \cdot \left(A_\gamma - A_{DBC1}\right) \quad (4)$$

$$\frac{dA_{DBC2}}{dt} = 1 + \sum\nolimits_{river,sediment,aerosol} \frac{\gamma}{A_{DBC2}} \cdot \left(A_\gamma - A_{DBC2}\right) \quad (5)$$

$$A_{DBC} = \frac{[DBC_1]}{[DBC]} \cdot A_{DBC1} + \frac{[DBC_2]}{[DBC]} \cdot A_{DBC2} \qquad (6)$$

Parameters are described in more detail in Supplementary Table 1. Three different scenarios are simulated and DBC age and concentration assessed: Simulation 1 includes both pools with first-order degradation rates as specified in [13], for example, with a turnover time on centennial (here: 100) and $>10^5$ (here: 10000) years. Loss due to photodegradation is only implemented for surfaces boxes, and the degradation rate constant is adjusted to achieve a total loss of 2-4 Tg DBC per year (Table 1). The intensity of the photoproduction scales with the fraction of UV light reaching the surface area of each box, with the distribution calculated using short-wave radiation data from the ERA5 reanalysis as in [14,15]. Input of DBC comes from rivers, distributed according to latitude as in [2]. Simulation 2 includes sources and sink processes as in simulation 1, and an additional input of pre-aged sediment for pool DBC_2 in the subsurface box. Uncertainties range over several orders of magnitude for this flux. To address this large uncertainty, an additional simulation was performed with a 10x larger sediment input flux. Simulation 3 includes sources and sink processes as in simulation 2, but an additional input of ages riverine input (for example, dissolution of PBC) and pre-aged DBC input from aerosols. Parameter values and prescribed fluxes for all simulations can be found in supplementary table 1.

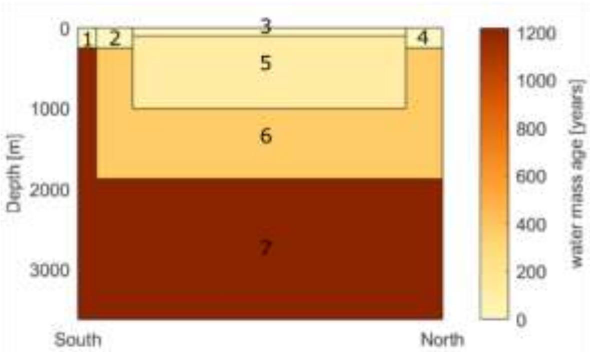

Supplementary Figure 1. Modelled ideal water mass age with the 7-box model, computed with static age 0 at the surface and aging upon transport to deeper waters with circulation in the model. Numbers indicate box numbers (compare supplementary table 2).

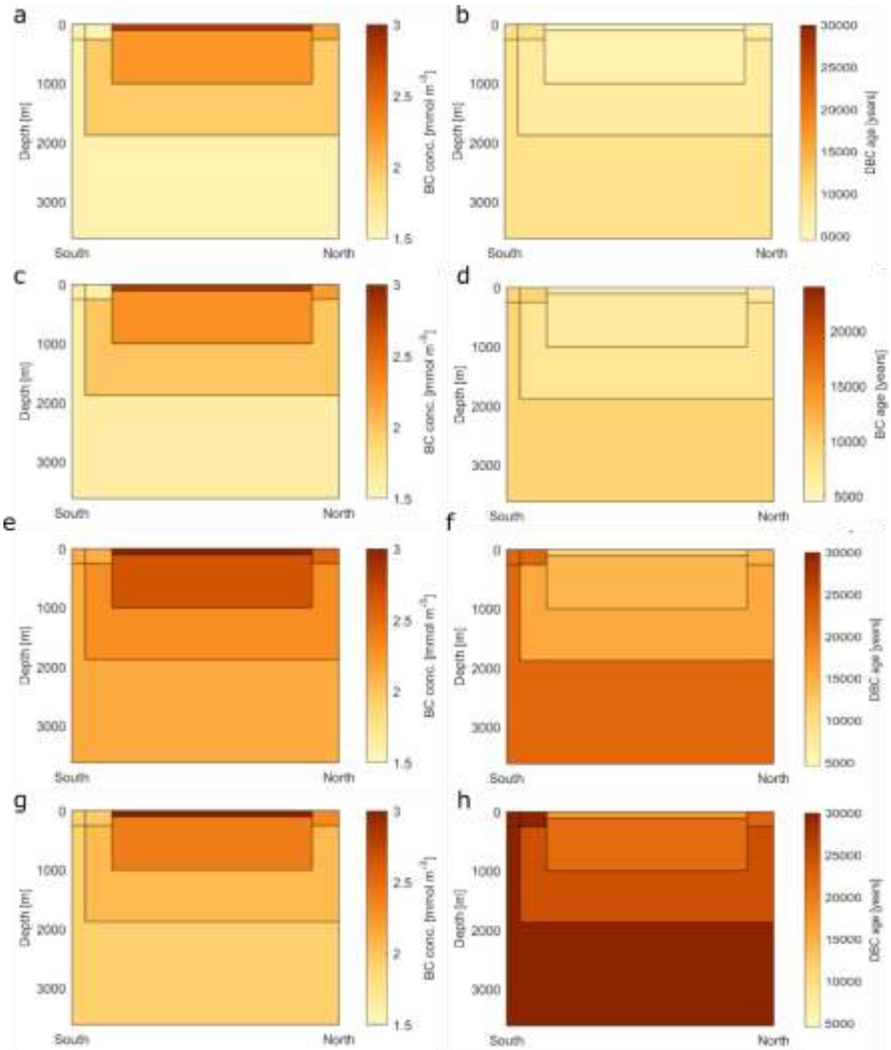

Supplementary Figure 2. Modelled DBC concentrations (left) and DBC ages (right) using the 7-box model. a) and **b)** simulation 1 with riverine input, UV loss at the surface and first-order chemical sinks of two DBC pools. **c)** and **d)** simulation 2 as in simulation 1 but with additional pre-aged sediment input, **e)** and **f)** simulation 2 but with 10x higher sediment input flux, **g)** and **h)** simulation 3 as in simulation 2 (high sediment flux) but with input of aerosols and dissolution of particle riverine flux at the surface.

Supplementary Table 1: Box model parameters and values. Values in [brackets] indicate individual values for boxes 1-7 (see supplementary figure 3 for box numbering).

Symbol	Parameter	Unit	Simulation 1	Simulation 2	Simulation 3
$[DBC_1]$	Concentration of DC pool 1 (fast overturning pool)	mmol C m^{-3}	Prognostic variable	Prognostic variable	Prognostic variable
$[DBC_2]$	Concentration of DC pool 1 (fast overturning pool)	mmol C m^{-3}	Prognostic variable	Prognostic variable	Prognostic variable
A_{DBC1}	Age of DBC pool 1	yr	Prognostic variable	Prognostic variable	Prognostic variable
A_{DBC2}	Age of DBC pool 2	yr	Prognostic variable	Prognostic variable	Prognostic variable
γ_{river}	DBC flux from rivers to DBC pool 1	Tg yr^{-1}	Total: 18 Tg [0 0 16.2 1.8 0 0 0]	Total: 18 Tg [0 0 16.2 1.8 0 0 0]	Total DBC: 18 Tg [0 0 16.2 1.8 0 0 0] Total DBC from PBC (assumed additional 10% with similar distribution): 1.8 Tg [0 0 1.62 0.18 0 0 0]
ε	Partitioning factor for riverine sources between DBC pool 1 and 2	-	0.7 (manually optimized)	0.7 (manually optimized)	0.8 (manually optimized)
$A_{\gamma river}$	Age of riverine input	yr	0	0	DBC: 0 DBC from PBC: 3700 yr
$\gamma_{sediment1}$	DBC flux from sediments to DBC pool 1	Tg yr^{-1}	-	0	0
$\gamma_{sediment2}$	DBC flux from rivers to DBC pool 2	Tg yr^{-1}	-	0.12 Tg yr^{-1} & 1.2 Tg yr^{-1}	1.2 Tg yr^{-1}
$A_{\gamma sediment}$	Age of sediment input	yr	-	50000 yr	50000 yr
$\gamma_{aerosol1}$	DBC flux from rivers to DBC pool 1	Tg yr^{-1}	-	-	0
$\gamma_{aerosol2}$	DBC flux from rivers to DBC pool 2	Tg yr^{-1}	-	-	Total: 1 Tg yr^{-1}, distributed evenly according to surface area of box)

$A_{y aerosol}$	Age of aerosol input	yr	-	-	50000 yr
k_1	Rate constant first order sink pool DBC1	yr^{-1}	0.01	0.01	0.01
k_2	Rate constant first-order sink pool DBC2	yr^{-1}	0.0001	0.0001	0.0001
λ_{UV}	Rate constant for photodegradation (multiplied by UV scaling factor)	yr^{-1}	0.04 x [0.035 0.042 0.862 0.0605 0 0 0] (optimized to yield an integrated annual loss of 3.5 Tg C, Table 1)	0.04 x [0.035 0.042 0.862 0.0605 0 0 0] (optimized to yield an integrated annual loss of 3.5 Tg C, Table 1)	0.04 x [0.035 0.042 0.862 0.0605 0 0 0] (integrated annual loss of 3.3 Tg C)

References

1 Wagner, S. *et al.* Isotopic composition of oceanic dissolved black carbon reveals non-riverine source. *Nature Communications* **10**, 5064, doi:10.1038/s41467-019-13111-7 (2019).

2 Jones, M. W. *et al.* Fires prime terrestrial organic carbon for riverine export to the global oceans. *Nature Communications* **11**, 2791, doi:10.1038/s41467-020-16576-z (2020).

3 Drake, T. W. *et al.* Du Feu à l'Eau: Source and Flux of Dissolved Black Carbon From the Congo River. *Global Biogeochemical Cycles* **34**, e2020GB006560, doi:https://doi.org/10.1029/2020GB006560 (2020).

4 Wagner, S. *et al.* Investigating Atmospheric Inputs of Dissolved Black Carbon to the Santa Barbara Channel During the Thomas Fire (California, USA). *Journal of Geophysical Research: Biogeosciences* **126**, e2021JG006442, doi:https://doi.org/10.1029/2021JG006442 (2021).

5 Liu, J. & Han, G. Tracing Riverine Particulate Black Carbon Sources in Xijiang River Basin: Insight from Stable Isotopic Composition and Bayesian Mixing Model. *Water Research* **194**, 116932, doi:https://doi.org/10.1016/j.watres.2021.116932 (2021).

6 Stubbins, A., Niggemann, J. & Dittmar, T. Photo-lability of deep ocean dissolved black carbon. *Biogeosciences* **9**, 1661-1670, doi:10.5194/bg-9-1661-2012 (2012).

7 Trilla-Prieto, N., Vila-Costa, M., Casas, G., Jiménez, B. & Dachs, J. Dissolved Black Carbon and Semivolatile Aromatic Hydrocarbons in the Ocean: Two Entangled Biogeochemical Cycles? *Environmental Science & Technology Letters* **8**, 918-923, doi:10.1021/acs.estlett.1c00658 (2021).

8 Allen Kylie, D. *et al.* Biogenic formation of amorphous carbon by anaerobic methanotrophs and select methanogens. *Science Advances* **7**, eabg9739, doi:10.1126/sciadv.abg9739.

9 Mentges, A. *et al.* Microbial Physiology Governs the Oceanic Distribution of Dissolved Organic Carbon in a Scenario of Equal Degradability. *Frontiers in Marine Science* **7**, doi:10.3389/fmars.2020.549784 (2020).

10 Toggweiler, J. R. Variation of atmospheric CO2 by ventilation of the ocean's deepest water. *Paleoceanography* **14**, 571-588, doi:https://doi.org/10.1029/1999PA900033 (1999).

11 Khatiwala, S. A computational framework for simulation of biogeochemical tracers in the ocean. *Global Biogeochemical Cycles* **21**, doi:https://doi.org/10.1029/2007GB002923 (2007).

12 Khatiwala, S., Primeau, F. & Holzer, M. Ventilation of the deep ocean constrained with tracer observations and implications for radiocarbon estimates of ideal mean age. *Earth and Planetary Science Letters* **325-326**, 116-125, doi:https://doi.org/10.1016/j.epsl.2012.01.038 (2012).

13 Coppola, A. I. & Druffel, E. R. M. Cycling of black carbon in the ocean. *Geophys. Res. Lett.* **43**, 4477 (2016).

14 Hersbach, H., Bell, B., Berrisford, P., Biavati, G., Horányi, A., Muñoz Sabater, J., Nicolas, J., Peubey, C., Radu, R., Rozum, I., Schepers, D., Simmons, A., Soci, C., Dee, D., and Thé- & paut. (2018).

15 Lennartz, S. T., Gauss, M., von Hobe, M. & Marandino, C. A. Monthly resolved modelled oceanic emissions of carbonyl sulphide and carbon disulphide for the period 2000–2019. *Earth Syst. Sci. Data* **13**, 2095-2110, doi:10.5194/essd-13-2095-2021 (2021).